Geotechnical Assessment Using Kinematic Analysis for an Unstable Road Cut, Along Haibat Sultan Mountain, Iraqi Kurdistan Region

Varoujan K. Sissakian (f.khajeek@ukh.edu.krd)
University of Kurdistan Hewler, ORCID No
Mark J. Vanarelli
University of Kurdistan Hewler
Hamed M. Jassim
Tishk International University, ORCID No
Hassan O. Omer
University of Kurdistan Hewler

Research Article

Keywords: Slope failure, Landslide, Kinematic analysis, Factor of Safety, Kurdistan Region

Posted Date: June 16th, 2022

DOI: https://doi.org/10.21203/rs.3.rs-1737686/v1

Abstract

There are many hazardous roads in the Iraqi Kurdistan Region (IKR) which traverse through mountainous terrains. One of these roads was selected for a geotechnical assessment in this paper. The road crosses the Haibat Sultan Mountain, north of Koya town in IKR; it is one of the most dangerous roads in this region. Annually, traffic is blocked by various types of slope failures along this road. There are numerous observed examples where bedding planes in the slope face daylight next to the road. To assess the road geotechnically, several stations of the Haibat Sultan Crossing road were studied to determine their stability using the Kinematic Analysis Method. A total of 11 stations were identified with the highest potential for slope failure. It was determined that only four stations (Nos. 4, 5, 7 and 9) could be evaluated using kinematic analyses. The kinematic analyses for the four stations were performed using DipAnalyst 2.0 software. The analyses identified the potential failure areas and their factors of safety (F.S.). The factors of safety at these four stations were calculated and ranged between 0.66 – 0.85 indicating unstable slopes. Based on this information, remedial measures were recommended at these locations and along associated sections of the road.

1. Introduction

The road crossing Haibat Sultan Mountain, north of Koya town in Iraqi Kurdistan Region (IKR) shows several examples of slope instability. This is mainly due to haphazard road construction without consideration for the geological conditions and constraints such as the type of the rocks, the hardness and thicknesses of the rock formations, the existence and orientation of bedding, joints, fractures, faults, which all have an impact on the rock strength and the stability of the slopes.

Many studies deal with the problems of road instability. Different instructions, guidelines and published articles were reviewed for our assessments. Among those studies, but not limited to are: Markland (1972), Hocking (1976), Hoek and Bray (1981), Goodman (1989), Canadian Geotechnical Society (1992), Hetzberg (1996), Watts et al. (2003), Hack et al. (2003), Wyllie and Mah (2005), Shong (2010), Taherynia et al. (2014), City of GOLDCOAST (2016), Basahel and Matri (2017).

1.1. Location

The study area is located northeast of Erbil city, near the Town of Koya (Fig. 1) within IKR, central northern part of Iraq. The road climbs Haibat Sultan Mountain as a very steep single lane road with different types of slope failures occurring; mainly due to daylighting slopes which were formed because of haphazard road construction in steeply dipping limestone beds.

1.2. Aim

The main aim of this research work is to perform geotechnical assessments of the unstable slopes using Kinematic Analysis Methods and then recommend remedial measures to stabilize the slopes.

1.3. Previous Works

The slope instability problems along roads in IKR are not well studied, although a few studies do exist. These studies have been carried out specifically concerning the unstable slopes along the Haibat Sultan crossing road. Hamasour (1991) studied the unstable slopes in an M.Sc. thesis and presented and discussed the unstable parts of the road indicating planar landslides. Jassim et al. (2013 and 2014) studied the unstable slopes and considered the landslides and rock falls as the main mass movements' phenomenon present in the study area. They identified 14 study stations along the roadway and concluded that the possibility of sliding is high. Sidiq et al. (2016) studied a landslide that had occurred on 11//11/ 2015 and documented the details and causes of the landslide that was a large planar landside; they also gave recommendations for stabilizing the unstable areas. Ibrahim and Jassim (2018), presented a report about the unstable slopes along the road crossing. They identified 18 study stations with different mass movements phenomena and recommended proposals to keep the road stable. It is worth mentioning that all previous studies have never used kinematic assessment.

2. Materials Used And Methodology

To perform the current study, we have used the following data: Geological and topographical maps of different scales, Satellite images, relevant published articles, and reports. We have performed this research work in the following steps:

2.1. Field Investigation

First, a field investigation was conducted on the 9th of October 2017 in the studied area to identify the unstable parts of the slopes along the road at 11 studied stations which were divided into three sections (Fig. 1) where data was collected for the kinematic assessment as shown in Table (1).

2.2. Assessment Method

To assess the stability of the slopes, we have used kinematic analysis. In this method, we performed stereonet projection analysis in four sites (where rocks are exposed with clear bedding planes) to identify the relation between the direction of the slope (road cut) and the orientation (i.e., strike and dip) of the bedding and joint planes of the exposed rocks. The paper by Wyllie and Mah (2008) provided guidance in in the construction of four stereonet projections in our kinematic analysis.

Table 1
Brief field description of the 11 studied stations

Station No.	Road Section	Mass Movement	Observations
1	1	Soil Slump	Recent soil failure indication with scarps (30–50 cm).
2		Soil Creep	Old soil creep within slope sediments of coarse rock fragments; indicated by bended trees.
3	2	Soil Creep	Old soil creep within slope sediments of coarse rock fragments covering the bed rock; indicated by bended trees (Fig. 6)
4		Landslide	Daylight slope within carbonates of the Pila Spi Formation with indication of recent failure (Fig. 5).
5		Landslide	Daylight slope within carbonates of the Pila Spi Formation with indication of recent failure. Claystone beds occur with traces of slicken side (Fig. 7L).
6		Soil Slump	Recent soil slump within slope sediments with coarse rock fragments covering the bed rock.
7		Landslide	Daylight slope within carbonates of the Pila Spi Formation with indication of recent failure. Large caverns, which help water passage within the beds (Fig. 7R).
8	3	Rock fall and toppling	Recent and active fall of thinly bedded claystone, as scree along the slope.
9		Rock fall, toppling and wedge sliding	Recent and active fall of thinly bedded claystone, as scree along the slope. Two medium sized wedge sliding had occurred. On top of the slope large limestone blocks occur in critical equilibrium (Fig. 9R).
10		Rock fall and toppling	Recent and active fall of thinly bedded claystone, as scree along the slope. Large recently fallen masses are removed out of the slope.
11		Rock fall and toppling	Recent and active fall of thinly bedded claystone, as scree along the slope.

2.2.1. Construction of Stereographic Projections

Field data were collected only from four stations (Nos. 4, 5, 7 and 9), because no rock outcrops were found with clear bedding planes in the other studied stations. The details of the collected data are presented in Table (2). The data are used in the construction of the stereographic projections using Stereonet 10.0 software to indicate the relation between the road cut (slope face) direction and the orientation (i.e., dip and strike) of the joints and bedding planes at the four stations.

Table 2
Field data of the bedding and joint planes in four stations

Station No.	Road Cut (slope) Direction / Slope (Degree and direction)	Strike direction/ Dip amount and direction		
		Bedding	**Joint Set 1**	**Joint Set 2**
4	**120/ 75● SW**	124/ 32● SW	196/ 90●	114/ 60● SW
		120/ 44● SW	204/ 70● SE	112/ 90●
		120/ 50● SW	200/ 80● SE	131/ 49● SW
5	**115/ 65● SW**	102/ 52● SW	204/ 58● SE	118/ 58● SW
		124/ 48● SW	230/ 40● SE	120/ 52● SW
		112/ 55● SW	225/ 47● SE	127/ 55● SW
7	**123/ 71● SW**	110/ 36● SW	229/ 70● SE	116/ 58● SW
		124/ 48● SW	230/ 40● SE	136/ 65● SW
		122/ 42● SW	244/ 65● SE	120/ 57● SW
9	**129/ 60● NE**	128/ 43● SW	195/ 60● SE	119/ 52● SW
	219/ 68● NW	123/ 42● SW	224/ 70● SE	132/ 50● SW
		126/ 47● SW	203/ 52● SE	123/ 48● SW

2.2.2. Kinematic Analysis

The methods of Markland (1972), Hocking (1976), Hoek and Bray (1976) and Watts et al. (1981) have been used to conduct kinematic analysis for four selected stations, and stereonet projections were constructed to identify slope instability. The depth of the tension cracks and the height of the water in the cracks were measured in the field. The data collected for kinematic analysis are presented in Table (2), where the averages of the attitudes have been used.

To perform kinematic analysis, we obtained the following numerical data [18]:

Static friction angle = 31°, rock density = 25 KN/ m^3 and cohesion = 61 KN/ m^2.

Computerized analysis of the data was applied for the four stations using DipAnalyst 2.0 software, based on Hoek and Bray (1981) and Watts et al. (2006) methods which identify the possibility of planar failure. “If the dip vector (middle point of the great circle) of the great circle representing a discontinuity set falls within the shaded area (area where the friction angle is higher than slope angle), then a potentiality for a plane failure exists” (op. sit). This assumption is utilized in the four studied stations. Factors of safety (F.

S.) were calculated for each station location, where a limit equilibrium analysis was applied to calculate the F. S. A factor of safety value equals to 1 represents limiting condition. A value greater than 1 represents a stable slope, and a value less than 1 indicates an unstable slope (Canadian Geotechnical Society, 1992 and Wyllie and Mah, 2005). The toppling zone that satisfies Goodman's (1989) criteria was noted in each station indicating the toppling possibility as calculated using DipAnalyst 2.0 software. The Goodman's criteria can be represented mathematically as:

$\sigma_a = \sigma_{fat} \times (1 - \sigma_m / \sigma_{ts})$ (Hertzberg, 1996)

where: σ_a is the alternating stress, σ_{fat} is the fatigue limit for completely reversed loading, σ_m is the mean stress, and σ_{ts} is the ultimate tensile strength of the material.

3. Geological Setting

The available geological data concerning the studied area are briefly reviewed including geomorphology, tectonics and structural geology and stratigraphy.

3.1. Geomorphology

The main geomorphological feature is the outstanding long and continuous anticlinal ridge that forms the bulk of Haibat Sultan Mountain. The ridge is characterized by giant flatirons with heights ranging between (25 – 150) m. The southern slope of the ridge is the manifestation of the dip of the bedding planes of thickly, well bedded limestone, which exhibits many landslide cases.

3.2. Stratigraphy

The stratigraphic sequence of the exposed rocks at the studied area is briefly described, based on Sissakian and Al-Jibouri (2014). The geological map is presented in Fig. (2). The geological formations are described from the oldest to youngest as follows:

- **Kolosh Formation** (Paleocene): The formation consists of black fine clastics, with some limestone tongues, which represent the Khurmala Formation.

- **Gercus Formation** (Eocene): The formation consists of thinly bedded fine clastics.

- Pila Spi Formation (Upper Eocene): The formation consists of white to greyish white, well bedded limestone and dolostone with some yellowish white marly limestone.

- Fatha Formation (Middle Miocene): The formation consists of cyclic sediments. Each cycle consists of alternation of thick claystone, bedded, white limestone and grey gypsum.

- Injana Formation (Upper Miocene): The formation consists of cyclic sediments; each cycle consists of alternation of sandstone, siltstone, and claystone; reddish brown in color.

3.3. Tectonics and Structural Geology

The main ridge in the studied area represents the contact between the Low Folded Zone (in the south) and the High Folded Zone (in the north). Both zones are within the Outer Platform of the Arabian Plate as they are part of the Zagros Thrust – Fold Belt (Fouad, 2015). The ridge that forms Haibat Sultan Mountain is the southwestern limb of a small anticline called Bustana and continues eastwards to form the south western limb of a very wide anticline called Khalikan anticline. It is NW – SE trending (Fig. 2). The dip amount ranges between (33 – 71)° SW. The existing structural features like faults and anticlinal axes don't have any significant role on the stability of the slopes under consideration. However, the two main jointing sets are perpendicular to the bedding planes and to each other, and with the bedding planes play a significant role in the stability of the slopes.

4. Results

We have acquired the following results from the field investigation and the application of kinematic analysis of the raw data.

4.1. Description of the Road

The road climbs the southern face of the mountain through well bedded and hard carbonates of the Pila Spi Formation. Almost all the road that cuts through sections A – B and B – C (Fig. 1) exhibit bedding planes which daylight in the slope face. Seasonally, many slope failures have occurred resulting in traffic blockages. It is worth mentioning that on 30th April 2019 a large failure occurred near Station No. 7.

The road along the northern face (Section C – D) of the mountain runs through soft clastic rocks of the Gercus and Kolosh formations (Fig. 2). Although the dip of the beds is opposite to the slope; there are still some small unstable slopes along the road. The main types of mass movements along this section of road are rock falls, toppling and wedge failure.

4.2. Description and Kinematic Analysis of the Four Stations

A potential unstable planar block may form if ($\psi_A < \psi_f$), which dips at a flatter angle than the face.

where: ψ_A is the dip of the bedding plane,

ψ_f is the dip of the slope or the face.

The four stations (Nos. 4, 5, 7 and 9) are described herein and the results of the kinematic analyses are presented in Table (3). The factor of safety for each station is also presented in Table (3). The values of rock density, friction angle and cohesion were acquired from the geotechnical study of Koya tunnel, which is located 500 m west of the studied area within the same rocks and same geological conditions (Bosphorus Technical Consulting Corporation, 2012).

Station No. 4:

The kinematic analysis for this station shows: The amount of the slope angle is 75° and that of the dip of the bedding plane is 41°, since (ψA < ψf) (a Daylight slope); therefore, the possibility of the failure is high (marked by pink colour in Fig. 3). The analysis was performed using DipAnalyst 2.0 software. The sliding could be prevented by only cutting the slope at an angle less than 41°. The dip amount and direction of the discontinuity sets (joints 1 and 2) may also influence the stability. Plane sliding is less likely; if the dip direction of the discontinuity (αA) differs from the dip direction of the face (αf) by more than about 20°; |αA − αf| > 20°, i.e. αA − αf must be more than 20°. Accordingly, for the joint 1: |209° − 120°| =89°, and because 89° >20°, therefore joint 1 has no effect on the sliding. For joint 2 |121° − 120°| =1°, and because 1° < 20°, therefore, there is a main effect of joint 2 on the sliding. This assumption is according to [1 and 2]. The data in this station show that the friction angle is greater than slope angle and the discontinuities are within the shaded area (Fig. 3). Therefore, a potentiality for a planar failure exists. The calculated factor of safety for this station is 0.67 (Fig. 3 and Table 3).

Station No. 5:

The kinematic analysis shows that the dip of the bedding plane has moderate effect on sliding as ΨA (51°) < ψf (65°) and increasing the angle of the slope will lead to high possibility of sliding. The direction of the bedding plane has a major effect on sliding as |112 − 115| must be > 20°, and because 3° < 20°. The joint 2 also has a main effect on sliding as |121 − 115| must be > 20°, and because 6° < 20°. While joint 1 has no significant role in the failure, because |219 − 115| must be > 20° and because 104° > 20°. The analysis by DipAnalyst 2.0 software shows that there is a high possibility for sliding by the bedding plane and joint 2 as both are within the shaded area (Fig. 4). The factor of safety is 0.75 (Table 3), which indicates that sliding possibility is high (Fig. 4). At this station, toppling is not possible since the pole of the bedding plane is out of the toppling zone criteria (Goodman, 1989) (Fig. 4).

Station No. 7:

The kinematic analysis shows that the slope angle is almost equal to the dip of the bedding plane; thus, it has minor to moderate effect on the sliding along layers of rocks in this station. Increasing of the angle of the slope in the same direction of the bedding plane will trigger failure. The direction of the bedding plane and Joint 2 has a significant role in sliding as the difference in their direction to the direction of the Road cut (slope face) is less than 20°. Joint 1 has almost no effect on sliding (Fig. 5) because joint 1 is dipping to southeast while the bedding plane and road cut (slope face) are dipping southwest ward. The numerical analysis by DipAnalyst 2.0 software shows that the value of the factor of safety is 0.66 (Table 3). At this station, toppling is less possible since the pole of the bedding plane is almost on the limits of the toppling zone criteria (Goodman, 1989) (Fig. 5).

Station No. 9:

This station is within soft clastic rocks where the dip of the beds is opposite to the road cut slope.

The kinematic analysis shows that the slope face (Road cut 1), which is 129/60° NE has no effect on the sliding. However, the slope face (Road cut 2), which is 219/68° NW has significant effect on the sliding. Moreover, Joint 2, which is 124/50° SW plays a big role in the sliding (Fig. 6). The factor of safety is 0.85 (Table 3). This indicates that sliding is likely to occur in Joint 2 and Road cut 2. At this station, toppling is not possible since the pole of the bedding plane is out of the toppling zone criteria (Goodman, 1989) (Fig. 6).

planes are in green and blue colors; road cuts are in black color and the internal friction angle is in violet color. The pink area represents the critical area indicating potentiality for sliding. For 9 B, the road cut is in red color as great circle. The bedding planes (in red), joint planes (in green and blue), all are represented as poles, whereas the internal friction angle is in green. On **9 A**, the critical area is highlighted in pink color, whereas in **9 B** the critical area is determined by DipAnalyst 2.0 software. Note the similarity between the critical areas in both cases.

Table 3
Numerical data used in calculation of the factor of safety

Station No.	Slope face Dip direction/ dip amount	Discon-tinuity Dip direction/ dip amount	Height (m)	Rock Density (Kn/m^3)	Friction Angle (●)	Cohe-sion (Kn/m^2)	Tension Cracks (Depth/ height of water) (cm)	Factor of Safety
4	210/ 75●	209/ 66●	43	25	31	61	50/ 2	**0.67**
5	205/ 65●	211/ 55●	44	25	31	61	70/ 4	**0.75**
7	213/ 71●	214/ 60●	68	25	31	61	70/ 5	**0.66**
9	309/ 68●	200/ 60●	56	19.55	22	58	20/ 1	**0.85**

5. Discussion

The results from the current study indicate that unstable slopes exist along the studied part of the road representing potential areas for landslides. To facilitate the discussion, the studied part of the road cut was divided into three sections. Section A – B, B – C, and C – D (Fig. 1).

Section A – B consists of thick red claystone with very thin limestone and gypsum beds.

Sections B – C consists of thickly bedded and massive hard limestone beds and is the most problematic and dangerous section.

Section C – D consists of thinly, well bedded, reddish brown claystone with thin horizons of limestone.

5.1. Sections A – B and B – C

These include stations Nos. 1–7 (Fig. 1). The main reasons for the presence of landslides and potential areas for sliding are: **1)** The majority of the road cuts are almost parallel to the bedding planes of the Pila Spi Formation, which forms daylighting slopes (Fig. 7), **2)** Locally, claystone and/ or residual clayey soil form potential areas for sliding (Stations No. 1 and 2) (Fig. 8), especially when oversaturated by rain water, which will increase the pore water pressure. This will decrease the internal friction and cause sliding (Terzaghi, 1943 and Terzaghi et al., 1996), **3)** The carbonates of the Pila Spi formation, locally includes karst cavities (Fig. 7b), which accelerates water penetration in the slope causing the failure. Also, some claystone layers can produce lubricated sliding surfaces (Fig. 9a).

The stereographic projections show that, in section B – C, the road cuts will be unstable unless the angle of the road cut slopes are made less than the dip amount of the exposed rocks along the road.

5.2. Section C – D

This section includes stations No. 8–11 (Fig. 1). No sliding can occur along the main road cut in this section. However, when the face of any road cut runs almost perpendicular to the slope of the main road cut; then sliding may occur (Fig. 6). The main mass wasting, which occurs along the road is in the form of rock disintegration (Fig. 10a and 11b).

From the kinematic analysis, we found that the slope of road cut and the attitude of the bedding and joints 1 and 2 are the main reasons for the sliding (Figs. 3, 4, 5, and 6).

This is attributed to: **1)** The claystone beds within the Gercus Formation are thinly bedded and intensely jointed (Fig. 10a); therefore, these areas are prone to disintegrate; even though the road runs along slopes, which are opposite to the dip direction, **2)** The directions of the road cuts and their slope angles intersect with the attitudes of the bedding and joint planes and form unstable slopes, and/ or prone areas for wedge failure (Fig. 10a), and **3)** The anti-dip slope is capped by the carbonates of the Pila Spi Formation forming hanging cliffs (Fig. 10b) because of the weathering of the soft rocks of the Gercus Formation, thus forming unstable slopes, which may exhibit toppling, sliding and occasionally rock fall.

The sliding masses in section B – C are large; up to more than one cubic meter (Fig. 11a), whereas in section C – D, the mass wasting is in the form of very small pieces (Fig. 11b). This is attributed to the exposed Pila Spi Formation (Massive limestone beds) in the former, whereas the Gercus Formation (Thinly bedded soft claystone beds) is exposed in the latter (Sissakian and Al-Jibouri, 2014) .

6. Conclusions

The calculated factor of safety in the four studied stations ranges between 0.66 – 0.85, indicating that the four stations (Nos 4, 5, 7 and 9) are not safe. Many of the slopes along the studied road cuts are unstable. Sections A – B suffers from soil failure within the residual soil and/ or the highly weathered claystone beds of the Fatha Formation. Section B – C suffers from landslides of large carbonate masses of the Pila Spi Formation. Whereas section C - D suffers from mass wasting with occasional wedge failure due to the presence of soft, well bedded and intensely jointed claystone beds of the Gercus Formation; therefore, the mass wasting products are in the form of small rock fragments (chips).

Recommendations

The results for the four stations (Nos 4, 5, 7 and 9) showed factors of safety ranging between 0.66 through 0.85. A factor of safety below 1.0 would produce failure of the slope or the situation where failure is imminent. All results were unacceptable since the factors of safety are below 1.0. Typically, factors of safety that represent acceptable design criteria in geotechnical engineering are established as a minimum of 1.5 which is 50 percent above the minimum factor of safety of 1.0. The following recommendations are meant to increase the factor of safety and reduce the possibility of slope failure. **Construction of:** 1) ditches that are lined with impervious material on the upper part of the unstable slopes to decrease water infiltration into the rock and/or soil, 2) ditches that are lined with impervious material at the base of the slopes facing the paved road to drain rainwater away from the road and decrease the infiltration of the water into the rocks and soil, 3) rock fall barriers along the slopes which are covered by the soft rocks of the Gercus Formation in the anti-dip slope side (i.e. section B – C). **Installation of:** 1) rock bolts in the limestone beds of the Pila Spi Formation, which form daylighting slopes, in section B – C, 2) steel dowels and concrete buttresses at selected locations in the section B – C, 3) horizontal drains in the slope of section (A – B) to reduce pore water pressure at specific locations, 4) retaining walls between the slope and the road along section B – C. **Applying** shotcrete along the slopes which are covered by soft rocks at specific locations. Removing of all rock dumped on the dip-slope side of the road, opposite the toe of the slope. **Maintaining of** offsets or construct additional offsets between the road and the toe of the slope in the section B – C.

Declarations

Conflicts of interest/Competing interests

All four authors of this manuscript declare that they haven't any conflicts of interest, as far as this manuscript is concerned.

Ethics approval

All four authors approve of and totally adhere to the publication ethics of the Arabian Journal of Geosciences

Consent to participate

All four authors of this manuscript declare that they have contributed to conducting the research work and accordingly writing this manuscript.

Consent for publication

All four authors of this manuscript declare that they have agreed upon submitting this manuscript for publication in the International Journal of Earth Sciences.

Availability of data and material

All used data are presented in 3 tables that are included in the manuscript.

Code availability

We have used DipAanalyist 2.0 software, based on Hoek and Bray (1981) and Watts (2003).

Authors' contributions

All authors contributed to the study conception and design. Material preparation, data collection and analysis were performed by all four authors. The first draft of the manuscript was written by Mr. Varoujan Sissakian. Dr. Mark Vanarelli, Dr. Hamed Jassim and Mr. Hassan Omer commented on previous versions of the manuscript and amended it scientifically and linguistically. All authors contributed to the field work and have read and approved the final manuscript. The four stereonet graphics and application of DipAnalyist 2.0 software was performed by Mr. Hassan Omer.

References

1. Basahel H, Metri H (2017) Application of rock mass classification systems to rock slope stability assessment: A case study. J Rock Mech. Geotec. Eng., 9 (6): 993 – 1009.
2. Bosphorus Technical Consulting Corporation (2012). Design of Haibat Sultan Tunnel and Approach Roads Report. The Ministry of Housing and Constructions, Erbil. General Directorate of Roads and Bridges, Erbil, Iraq.
3. Canadian Geotechnical Society (1992) Canadian Foundation Engineering Manual, BiTech Publishers Ltd., Vancouver, Canada.
4. City GOLDCOAST (2016) Geotechnical Stability Assessment Guidelines (2016). Internet data. http://www.goldcoast.qld.gov.au/documents/bf/geotechnical_stability_guidelines.pdf
5. Fouad SF (2015) Tectonic Map of Iraq, scale 1:1000000, 3rd Edition. Iraqi Bull. Geol. Min., 15 (1): 1 – 8.
6. Goodman RE (1989) Introduction to Rock Mechanics. 2nd Edition, John Wiley and Sons, Hoboken.
7. Hack R, Price D, Rengers N (2003) A new approach to rock slope stability-a probability classification (SSPC). Bulletin of Engineering Geology and the Environment, 62(2):167 – 184. https://hack.home.xs4all.nl/ WORKHack/ Publications/ 2003% 20sspc/SSPC%20ver%20web.pdf.

8. Hamasour Gh A (1991) Engineering – Geological study of rock slope stability in Haibat Sultan area, NE Iraq. Unpublished M.Sc. Thesis, University of Salahaddin, Erbil, Iraq.
9. Hertzberg RW (1996) Deformation and Fracture Mechanics and Engineering Materials. John Wiley and Sons, Hoboken, NJ.
10. Hocking GA (1976) Method for distinguishing between single and double plane sliding of tetrahedral wedges. International Journal of Rock Mechanics and Mining Sciences, Vo. 13, No.7. www.sciencedirect.com/science/article/pii/S.... (1976).
11. Hoek E, Bray JW (1981) Rock Slope Engineering, 3rd edition. The Institute of Mining and Metallurgy, London, England, 358 pp. www.scirp.org/ (S(oyulxb452alnt1aej1nfow45))/ reference/....
12. Ibrahim ZJ, Jassim HM (2017) Slope Stability Study at Haibat Sultan Road / Kurdistan Region-Iraq, Individual Project Report, University of Kurdistan Hewler (UKH), Erbil, Iraq.
13. Jassim HM, Saad SA, Ghafour BD (2013) Slope stability assessment along the Haibat Sultan main road, Koya, Kurdistan. Proceedings of First International Symposium on Urban Development, Koya, Iraq.
14. Jassim HM, Rasheed ZN, Ghafour BD, Ahmed FR (2014) On the Landslide of Daigala Slope-Kurdistan-Iraq. IJETT, 12 (10): 503 – 509.
15. Markland JTA (1972) Useful technique for estimating the stability of rock slopes when the rigid wedge sliding type of failure is expected. Imperial College Rock Mechanics Research Report No. 19, 10 pp.
16. Shong LS (2010) Slope Stability Assessment. G&P Geotechnics Sdn Bhd. http:// www. gnpgeo.com.my/download/publication/L2.pdf
17. Sidiq SA, Muhmed AS, Haris GK, Hamma DM, Abdullah MM, Bibani HH, Muhealldin HK, Mustafa HA, Sissakian VK, Al-Ansari N (2016) Mechanism of Haibat Sultan Mountain Landslide in Koya, North Iraq. Engineering, 8: 535 – 544. http//:www.Scrip.org./journal/eng. http//:dx.doi.org/10.4236/eng.2016.880550.
18. Sissakian VK, Al-Jibouri BM (2014) Stratigraphy: In Geology of the High Folded Zone. Iraqi Bull. Geol. Min., Special Issue, 6: 73 – 161.
19. Sissakian VK, Fouad SF (2014) Geological Map of Erbil and Mahabad Quadrangles, scale 1:250000, 2nd Edition. Iraq Geological Survey Publications, Baghdad, Iraq.
20. Taherynia MH, Mohammadi M, Ajalloeian R (2014) Assessment of Slope Instability and Risk Analysis of Road Cut Slopes in Lashotor Pass, Iran. J. Geol. Res., Vol. 2014, Article ID 763598, 12 pp , (2014). http://dx.doi.org/10.1155/2014/763598
21. Terzaghi K (1943) Theoretical Soil Mechanics. John Wiley and Sons. com/doi/ 10.1002/9780470172766.fmatter/pdf
22. Terzaghi K, Peck RB, Mesri Gh (1996) Soil Mechanics in Engineering Practice. John Wiley and Sons. https://www.abebooks.com/.../soil-mechanics-in-engineering-practice/.../terzaghi-karl

23. Watts CF, Gilliam DR, Hrovatic MD, Hong H (2003) User's Manual - ROCKPACK III for Windows, C.F.Watts and Associates, Radford, VA, USA, 33 pp.
24. Wyllie DC, Mah CW (2005) Rock Slope Engineering, Civil and Mining, 4th edition. Spon Press is an imprint of the Taylor & Francis Group. Retrieved from https://civilenglineering.files.wordpress.com/2014/10/rock_slope_engineering_civil_andmining.pdf

Figures

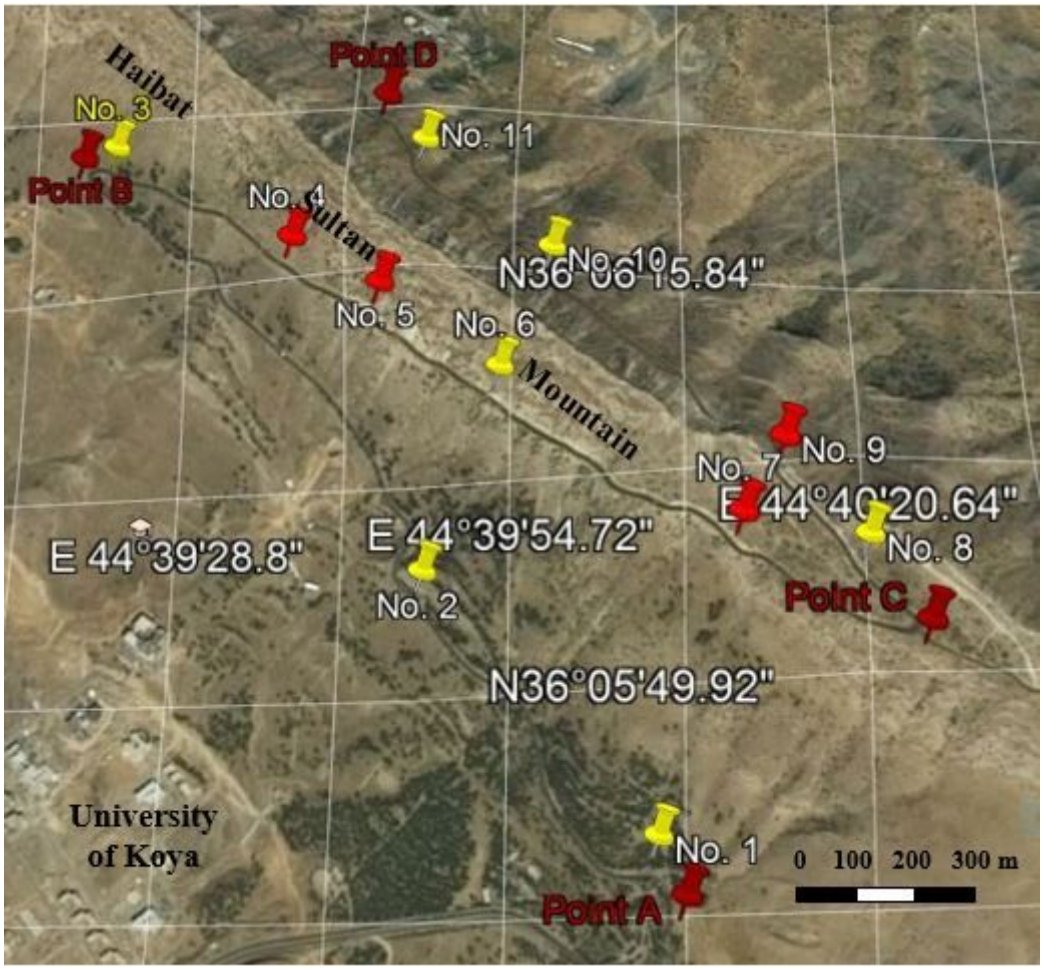

Figure 1

Satellite image of the studied part of Haibat Sultan crossing road (studied stations are in red, in yellow are the numbers of the road's three parts)

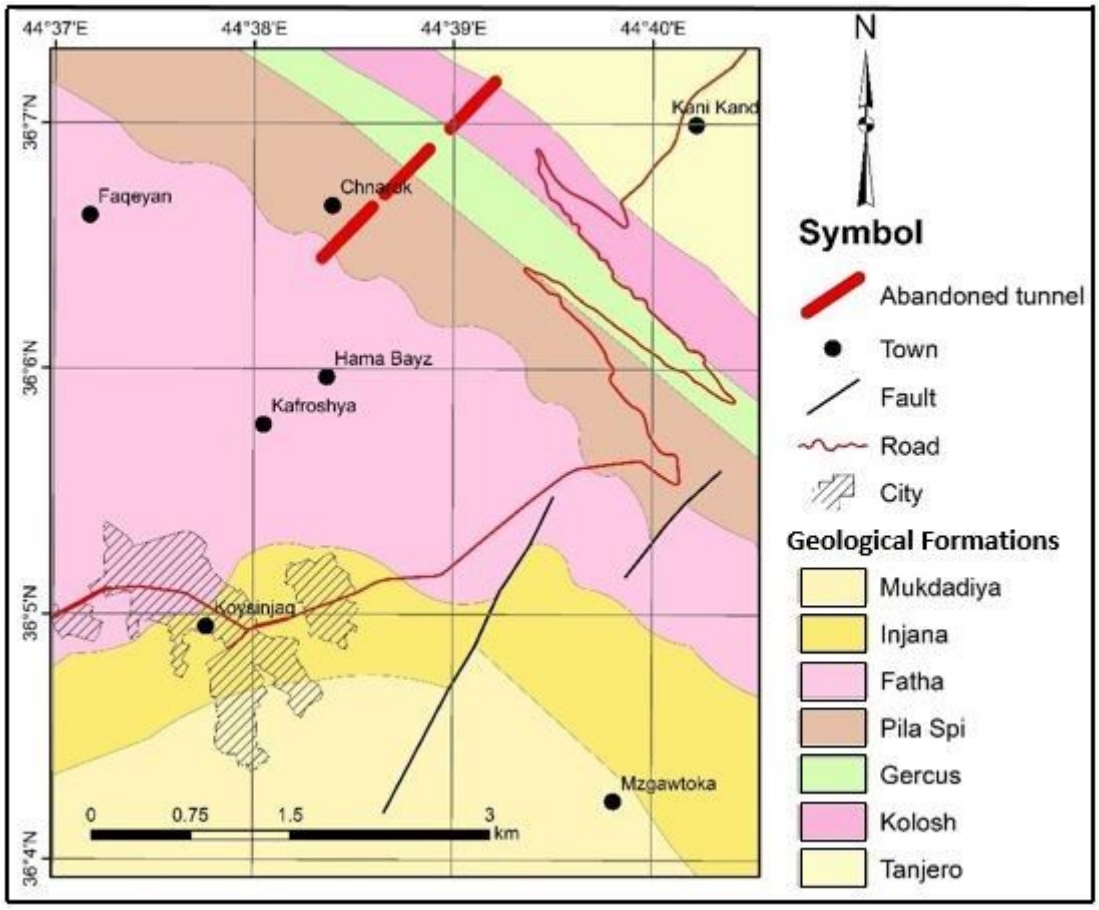

Figure 2

Geological Map of the study area (Modified from Sissakian and Fouad, 2014)).

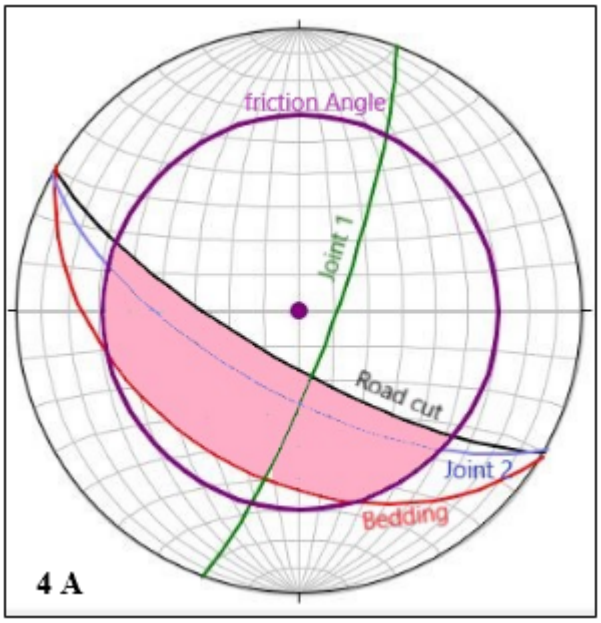

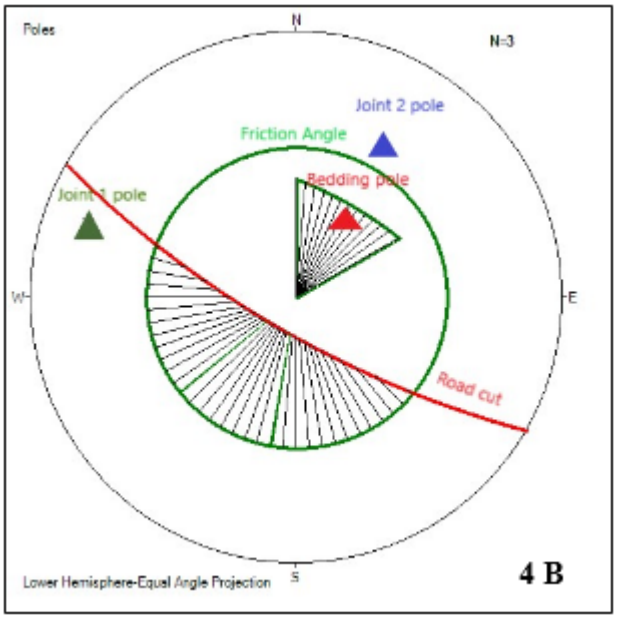

Figure 3

Stereographic projections of stations No. 4. For 4 A, the bedding plane is in red color, joint planes are in green and blue colors, road cut is in black color and the internal friction angle is in violet color. The pink area represents the critical area indicating potentiality for sliding. For 4 B, the road cut is in red color as great circle. The bedding planes (in red), joint planes (in green and blue), all are represented as poles, whereas the internal friction angle is in green. On **4 A**, the critical area is highlighted, whereas in **4 B** the critical area is determined by DipAnalyst 2.0 software. Note the similarity between the critical areas in both cases.

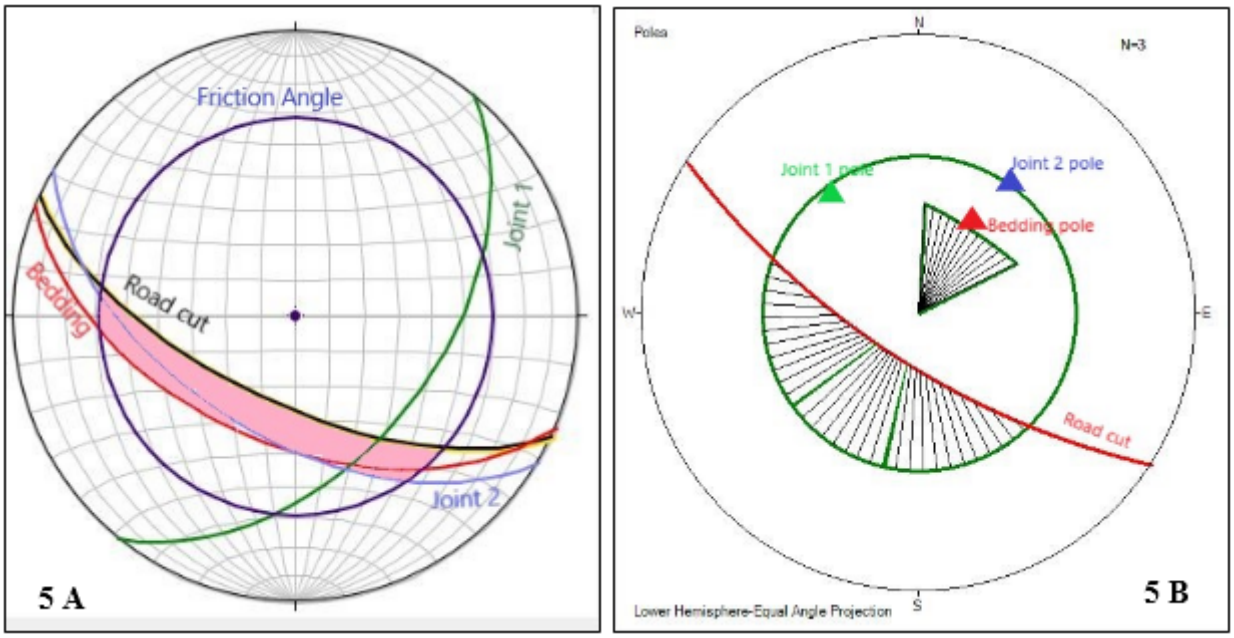

Figure 4

Stereographic projections of station No. 5. For 5 A, the bedding plane is in red color, joint planes are in green and blue colors, road cut is in black color and the internal friction angle is in violet color. The pink area represents the critical area indicating potentiality for sliding. For 5 B, the road cut is in red color as great circle. The bedding plane (in red), joint planes (in green and blue), all are represented as poles, whereas the internal friction angle is in green. On **5 A**, the critical area is highlighted, whereas in **5 B** the critical area is determined by DipAnalyst 2.0 software. Note the similarity between the critical areas in both cases.

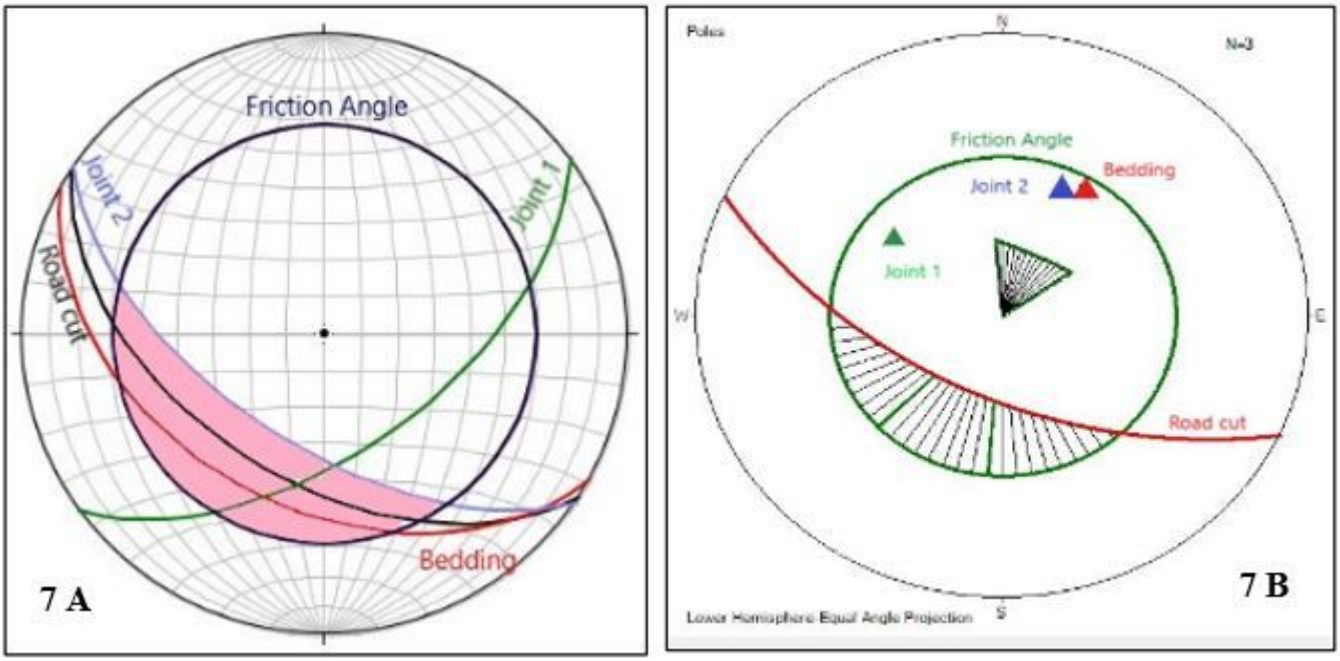

Figure 5

Stereographic projections of station No. 7. For 7 A, the bedding plane is in red color, joint planes are in green and blue colors, road cut is in black color and the internal friction angle is in violet color. The pink area represents the critical area indicating potentiality for sliding. For 7 B, the road cut is in red color as great circle. The bedding plane (in red), joint planes (in green and blue), all are represented as poles, whereas the internal friction angle is in green. On **7 A**, the critical area is highlighted, whereas in **7 B** the critical area is determined by DipAnalyst 2.0 software. Note the similarity between the critical areas in both cases.

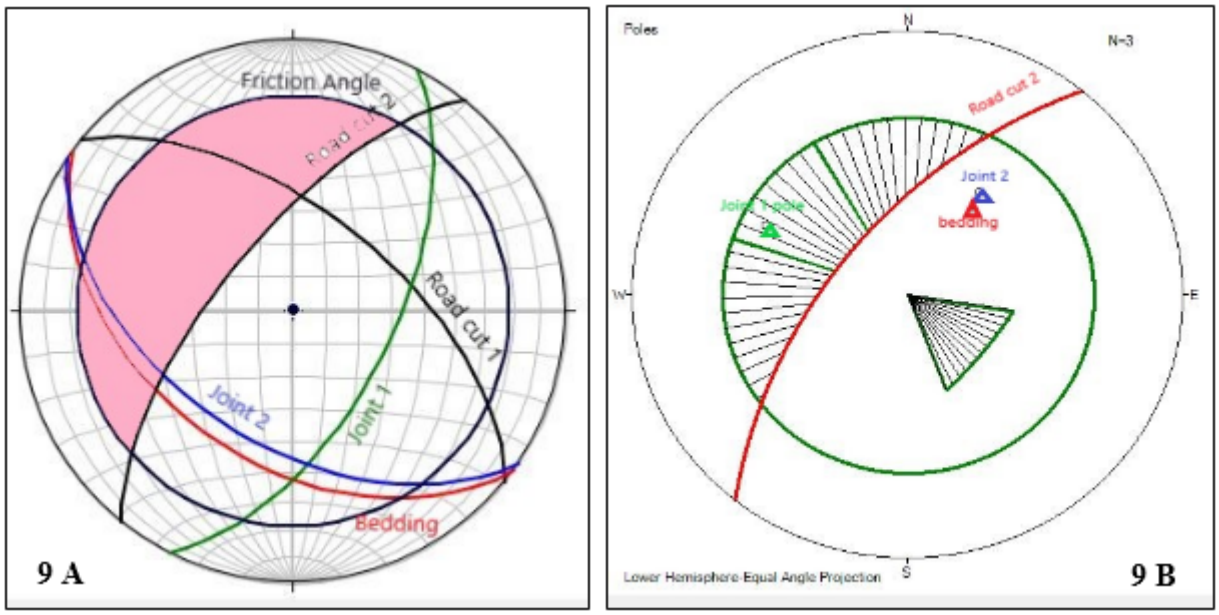

Figure 6

Stereographic projections of station No. 9. For 9 A, the bedding plane is in red color, joint

planes are in green and blue colors; road cuts are in black color and the internal friction angle is in violet color. The pink area represents the critical area indicating potentiality for sliding. For 9 B, the road cut is in red color as great circle. The bedding planes (in red), joint planes (in green and blue), all are represented as poles, whereas the internal friction angle is in green. On **9 A**, the critical area is highlighted in pink color, whereas in **9 B** the critical area is determined by DipAnalyst 2.0 software. Note the similarity between the critical areas in both cases.

Figure 7

Daylighting slopes of the well bedded rocks of the Pila Spi Formation. Note the unstable slopes due to road cuts, which are almost parallel to the dip of the beds (Station No. 7).

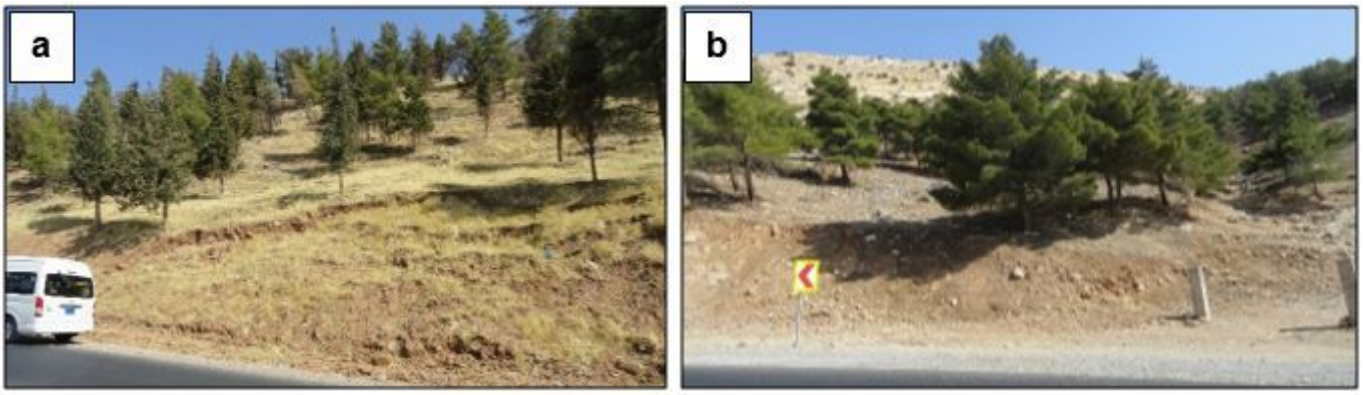

Figure 8

Two unstable slopes in residual soils. 8a Station No. 1, note the recent failure with

the developed cliff in the crown area. 8b Station No. 2, note the inclined trees.

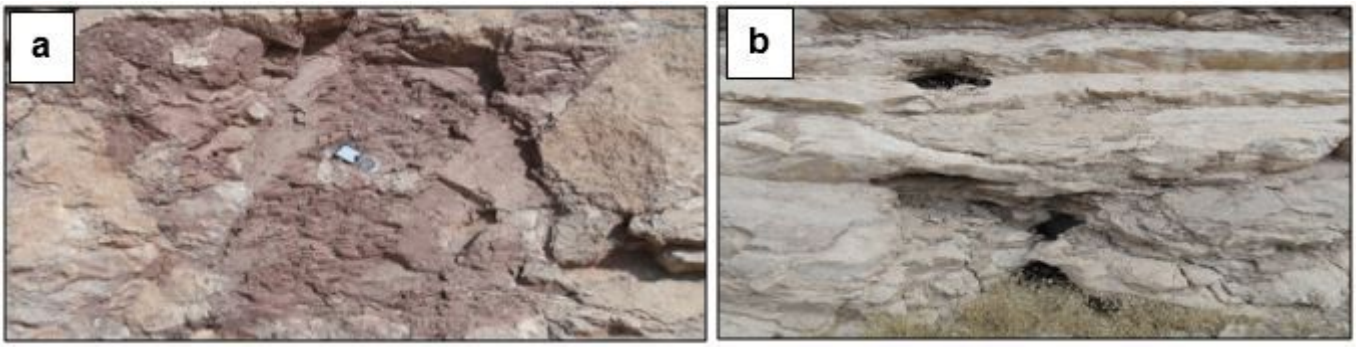

Figure 9

The Pila Spi Formation, 9a Reddish brown claystone, it acts as a lubricant surface for sliding after being oversaturated, 9b Karst cavities, which accelerate water penetration (Near Station No. 7).

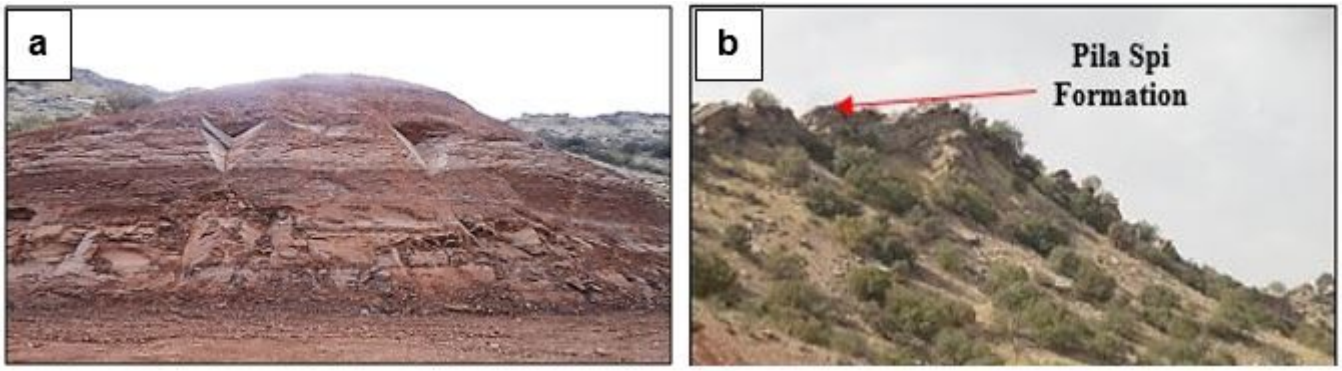

Figure 10

a. The Gercus Formation well bedded and intensely jointed claystone beds and the two-wedge sliding (Station No. 10), 10b Hanging cliffs formed by the carbonates of the Pila Spi Formation, overlying soft rocks of the Gercus Formation; forming prone areas for sliding, toppling and rock fall.

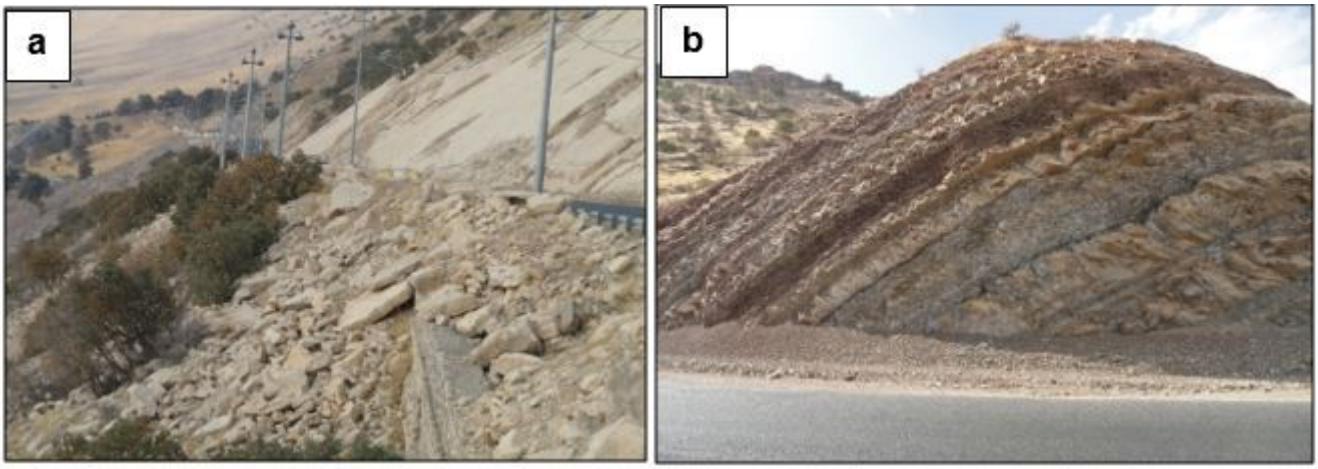

Figure 11

a. Remains of an old landslide of the Pila Spi Formation dumped down of landslide areas (Near Station No. 7). Note the size of the blocks and damaged parts of safety wall alongside the road, 11b Remains of mass wasting of thinly bedded claystone in the Gercus Formation (Station No. 11).